

4 Optimal Low-Thrust Transfer Using Variable Bounded Thrust

4.1 Introduction

The problem of minimum-fuel time-fixed orbit transfer and rendezvous using continuous low thrust, bounded from above and below, is analyzed here. The formulation is based on the use of the variation of parameters equations, which are written in terms of a set of nonsingular equinoctial elements, where the mean longitude represents the fast element. The consideration of maximum and minimum bounds on the thrust magnitude with constant power is equivalent to constraining the specific impulse of the propulsion system, such that this particular variable is optimized during the transfer. The thrust vector orientation is also optimized in order to minimize fuel consumption. Exact nonlinear dynamics for state vector propagation and constraint inequalities on the thrust magnitude are considered in the formulation of this low-thrust transfer problem.

Specific impulse or I_{sp} is no longer considered to be a fixed quantity during the transfer, and is now allowed to vary between user-defined minimum and maximum bounds, such that both thrust magnitude and direction are optimized to yield the overall minimum-fuel solution. Assuming that power remains constant, the thrust magnitude is inversely proportional to the specific impulse, which is continuously adjusted by varying the beam voltage. We first revisit the fundamentals of flight mechanics and low-thrust propulsion developed in [1–3], and derive the equivalent expression for the optimal controls for the thrust magnitude unconstrained case, using equinoctial elements instead of the usual Cartesian coordinates. The necessary conditions for optimality for the thrust-bounded case are derived following [4] and [5], and the problem of low-thrust transfer and rendezvous of [6–8] and Chapter 3 of this book extended to the case of continuously varying I_{sp} . An example of minimum-fuel time-fixed rendezvous with different I_{sp} bounds is solved numerically and compared with earlier results generated with constant thrust.

As the fixed transfer time approaches infinity, the solutions will approach the optimal multi-impulse chemical transfer solution with an infinite number of negligibly small thrust arcs replacing each impulse. In this case, the thrust magnitude will approach zero, and I_{sp} will approach infinity, or in practice, a lower and upper bound respectively. However, for finite transfer times, both the lower and upper bounds on the thrust magnitude will effectively act as constraints to shape the transfer trajectory, in order to minimize the fuel expenditure.

4.2 The Optimization of the Thrust Magnitude

From rocket propulsion fundamentals, and using Newton's law for a variable-mass body, the equation of motion of a rocket-powered vehicle is given by

$$m\ddot{\mathbf{r}} = \dot{m}\mathbf{c} + m\mathbf{g} \quad (4.1)$$

where \mathbf{r} is the vehicle position vector, \mathbf{g} is the acceleration of gravity, \mathbf{c} is the exhaust velocity, and $\dot{m} < 0$ is the rate at which mass is expelled from the engine. The thrust vector $\mathbf{f} = \dot{m}\mathbf{c}$ is directed opposite the exhaust velocity vector, such that the acceleration can be written as

$$\mathbf{a} = \frac{\mathbf{f}}{m} = \ddot{\mathbf{r}} - \mathbf{g} \quad (4.2)$$

For a solar electric-powered ion thruster, the exhaust stream or beam power can be written as

$$P_B = \frac{fc}{2} \quad (4.3)$$

and, because $f = -\dot{m}c$, it can be written as

$$P_B = \frac{f^2}{2\dot{m}} \quad (4.4)$$

It can also be expressed in terms of the beam voltage V_B and the beam current I_B as

$$P_B = V_B I_B \quad (4.5)$$

Equation (4.3) can be derived from the following two expressions based on electrostatics considerations

$$V_B e = \frac{m_i}{2} c^2 \quad (4.6)$$

$$I_B = \left(\frac{e}{m_i} \right) (-\dot{m}) \quad (4.7)$$

The first expression states that if a particle of mass m_i and charge e , and negligible initial velocity, passes through a potential difference V_B it will acquire a kinetic energy of $1/2 m_i c^2$, where c is the exhaust velocity. The second expression is the definition of the current such that the beam power P_B is written as

$$P_B = I_B V_B = \frac{1}{2} (-\dot{m}) c^2$$

and, because $f = -\dot{m}c$, then

$$P_B = \frac{1}{2} fc$$

Alternatively, from Equation (4.6), an expression relating the I_{sp} to the beam voltage can be obtained, because, with $c = I_{sp}g$

$$\begin{aligned} c &= \left[2 \left(\frac{e}{m_i} \right) V_B \right]^{1/2} \\ I_{sp} &= \frac{1}{g} \left[2 \left(\frac{e}{m_i} \right) V_B \right]^{1/2} \end{aligned} \quad (4.8)$$

For a given beam power P_B , the thrust versus mass flow rate curve of an ion rocket is parabolic, because, from Equation (4.4)

$$f = \sqrt{-2\dot{m}P_B} \quad (4.9)$$

This behavior is very different from that of a constant exhaust velocity rocket, because in the latter case the curve is linear

$$f = -\dot{m}c \quad (4.10)$$

Conversely, the mass flow rate expressions for both types of vehicle are

$$\dot{m} = -\frac{f}{c} \quad (4.11)$$

$$\dot{m} = \frac{-f^2}{2P_B} \quad (4.12)$$

It is therefore advantageous from a propellant consumption point of view to have high exhaust velocity or high power.

Furthermore, Equation (4.9) shows that the same level of thrust can be achieved by different combinations of \dot{m} and P_B because, if a lower power level is selected, an appropriate increase in \dot{m} will maintain f constant.

However, from Equation (4.12), and for a given f , it is seen that \dot{m} is at a minimum if P_B is chosen at its maximum level.

This means that at each instant of time the selection of P_B at its maximum value, namely $P_{B_{\max}}$, will achieve the required thrust for minimum \dot{m} or minimum fuel consumption. In other words, from all the possible ways of flying a required trajectory, meaning an acceleration time history $\mathbf{a}(t) = \ddot{\mathbf{r}}(t) - \mathbf{g}(t)$, the selection of $P_{B_{\max}}$ is the only one that results in minimum fuel expenditure [3].

Ion rockets must therefore always operate at $P_{B_{\max}}$. Then, it is clear from Equation (4.3), with $P_B = P_{B_{\max}}$, that as the thrust is decreased, I_{sp} will increase and vice versa. Because the I_{sp} is dependent on the beam voltage V_B , it can be obtained by adjusting V_B , provided that I_B is also adjusted to obtain the required $P_{B_{\max}}$ power, because $P_B = I_B V_B$. All these fundamental ideas are encapsulated in Figures 4.1, 4.2 and 4.3. In Figure 4.1, the thrust versus mass flow rate curve for a low-thrust rocket with constant exhaust velocity is depicted. Because c cannot be varied in this type of rocket, the thruster operates at f_{\max} only [3].

Figure 4.2 corresponds to the variable c case, with $f = (-2\dot{m}P)^{1/2}$ for a given P . The power levels below P_{\max} result in Region II, with Region I being completely inaccessible, because it corresponds to $P > P_{\max}$, which is impossible.

As pointed out by Marec [3], it is not optimal to operate these types of thrusters at a power level $P_1 < P_{\max}$, because for the same thrust f_1 , the operation at P_{\max} depicted by point 2 results in the minimum mass flow rate or propellant expenditure.

In Figure 4.3, and for a given P_{\max} , any operating point A corresponds to a unique combination of beam voltage V_B and beam current I_B . If V_B is increased, the I_{sp} or c will also increase according to Equation (4.8), and, because power is held at $P_{\max} = \text{constant}$, the thrust will decrease accordingly, because $P = 1/2fc$. Conversely, decreasing I_{sp} or V_B will result in increasing thrust and I_B .

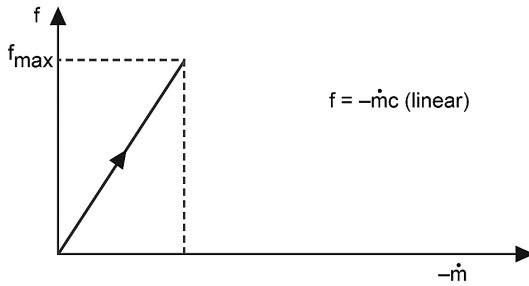


Figure 4.1 Thrust versus mass flow rate for a constant exhaust velocity.
 Source: [3].

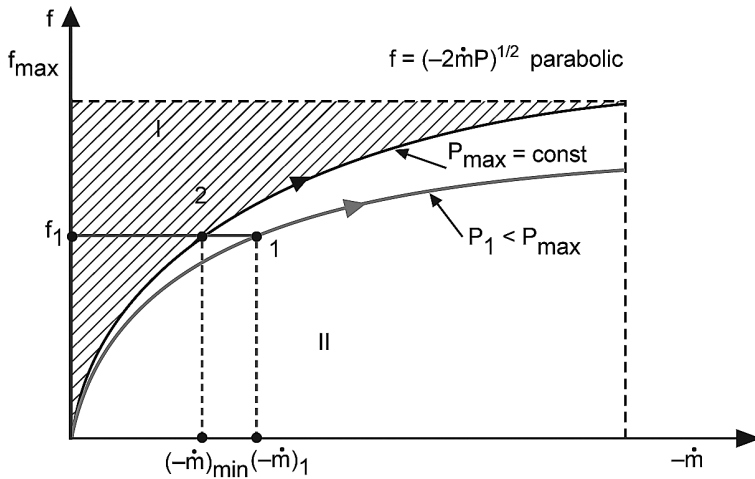


Figure 4.2 Selection of optimal thrust.
 Source: [3].

In Figure 4.4, the unreachable Region I is extended further by the inclusion of the boundary $00'$, which corresponds to the equation $f = -\dot{m}c_{\max}$, where c_{\max} is the maximum exhaust velocity achieved by the rocket. This boundary is necessary to prevent the exhaust velocity or the I_{sp} from growing to very large values, as the thrust is decreased toward its minimum value. This minimum is conveniently defined at point 0, such that the operating arc is the arc 03 on the P_{\max} parabola.

Edelbaum's analysis of the optimization of the thrust magnitude using the Cartesian formulation is first shown for the sake of completeness. This analysis is next translated to the formulation using the nonsingular equinoctial orbit elements, which is then extended to the case of constrained thrust magnitude. Following Edelbaum and letting \mathbf{r} and \mathbf{v} stand for the spacecraft position and velocity vectors, the second-order differential equation of motion is reduced to the following first-order form:

$$\dot{\mathbf{v}} = \frac{\mathbf{f}}{m} + \mathbf{g}(\mathbf{r}, t) \tag{4.13}$$

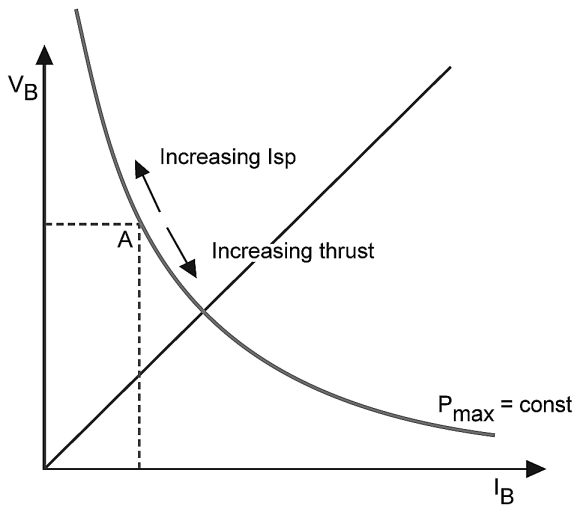


Figure 4.3 Beam voltage and current variation for a given power P_{max} .

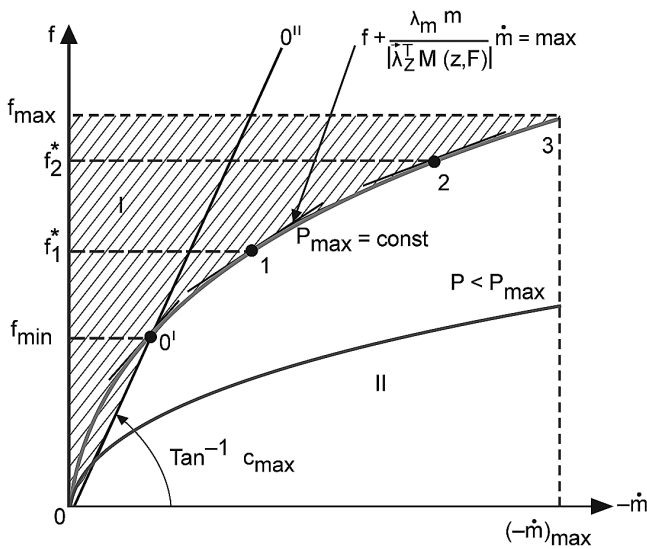


Figure 4.4 Thrust versus mass flow rate for a variable exhaust velocity rocket.
Sources: [1–3].

$$\dot{\mathbf{r}} = \mathbf{v} \tag{4.14}$$

with \mathbf{f} and \mathbf{g} representing the thrust and acceleration of gravity vectors, respectively. The mass flow rate obeys the general form

$$\dot{m} = \dot{m}(\mathbf{r}, t, \mathbf{f}) \tag{4.15}$$

The Hamiltonian of such a system is given by

$$H = \lambda_v \cdot \frac{\mathbf{f}}{m}(\mathbf{r}, t) + \lambda_v \cdot \mathbf{g}(\mathbf{r}, t) + \lambda_r \cdot \mathbf{v} + \lambda_m \dot{m}(\mathbf{r}, t, \mathbf{f}) \tag{4.16}$$

The Euler–Lagrange equations are therefore

$$\dot{\lambda}_v = -\frac{\partial H}{\partial \mathbf{v}} = -\lambda_r \quad (4.17)$$

$$\dot{\lambda}_r = -\frac{\partial H}{\partial \mathbf{r}} = -\frac{\lambda_v}{m} \cdot \frac{\partial \mathbf{f}}{\partial \mathbf{r}} - \lambda_v \cdot \frac{\partial \mathbf{g}}{\partial \mathbf{r}} - \lambda_m \frac{\partial \dot{m}}{\partial \mathbf{r}} \quad (4.18)$$

$$\dot{\lambda}_m = -\frac{\partial H}{\partial m} = \frac{\lambda_v \cdot \mathbf{f}}{m^2} \quad (4.19)$$

The application of Pontryagin's maximum principle requires that the control vector, namely the thrust vector \mathbf{f} , must be selected in such a manner as to maximize H at each instant of time. Because \mathbf{f} appears in \dot{m} , this necessary condition translates into

$$\frac{\lambda_v \cdot \mathbf{f}(\mathbf{r}, t)}{m} + \lambda_m \dot{m}(\mathbf{r}, t, \mathbf{f}) = \text{maximum} \quad (4.20)$$

This can be simplified further if \dot{m} is a function of thrust magnitude but not direction. This is the case of the unconstrained transfer with free yaw, pitch and roll. In these cases, $\dot{m} = \dot{m}(\mathbf{r}, t)$, such that the above condition reduces to

$$\frac{\lambda_v \cdot \mathbf{f}(\mathbf{r}, t)}{m} + \lambda_m \dot{m}(\mathbf{r}, t) = \text{maximum} \quad (4.21)$$

This requires that the thrust vector \mathbf{f} remains aligned with λ_v at all times, because $\lambda_v \cdot \mathbf{f}$ is then maximum. This results in

$$\frac{\lambda_v f}{m} + \lambda_m \dot{m} = \text{maximum} \quad (4.22)$$

From Equation (4.12), \dot{m} can be replaced by $-f^2/2P$, which reduces the expression in Equation (4.22) to

$$f - \frac{\lambda_v m}{2\lambda_v P} f^2 = \max \quad (4.23)$$

Maximizing this expression with respect to the thrust magnitude f results in

$$f^* = \frac{\lambda_v P}{\lambda_m m} \quad (4.24)$$

and from Equation (4.3), the optimal I_{sp}^* is then

$$I_{sp}^* = \frac{2P}{gf^*} = \frac{2m\lambda_m}{g\lambda_v} \quad (4.25)$$

Let us now carry out the optimization of f for the equinoctial formulation, using the equinoctial orbit elements represented by the vector $\mathbf{z} = (ahkpq\lambda)^T$ instead of the \mathbf{r} and \mathbf{v} formulation used above.

These nonsingular elements are defined as before in terms of the classical elements by the following relationships, namely $a = a$, $h = e \sin(\omega + \Omega)$, $k = e \cos(\omega + \Omega)$, $p = \tan(i/2) \sin \Omega$, $q = \tan(i/2) \cos \Omega$ and $\lambda = M + \omega + \Omega$, with λ standing for the mean longitude. Letting $\hat{\mathbf{u}}$ represent a unit vector in the direction of the thrust, the variation of

parameters equations for the thrust perturbation are given by Equation (4.26) with the addition of an n term to $\dot{\lambda}$. Here, n stands for the orbit mean motion at the current time t :

$$\dot{\mathbf{z}} = \left(\frac{\partial \mathbf{z}}{\partial \dot{\mathbf{r}}} \right) \hat{\mathbf{u}} f_t = M \hat{\mathbf{u}} f_t \tag{4.26}$$

$f_t = f/m$ represents the instantaneous perturbation acceleration with $\partial \mathbf{z} / \partial \dot{\mathbf{r}}$ and $\hat{\mathbf{u}}$ expressed in the direct equinoctial frame defined in [7] and Chapter 3 of this book. The M matrix above is given as before by

$$\frac{\partial a}{\partial \dot{\mathbf{r}}} = 2a^{-1}n^{-2} (\dot{X}_1 \hat{\mathbf{f}} + \dot{Y}_1 \hat{\mathbf{g}}) = M_{11} \hat{\mathbf{f}} + M_{12} \hat{\mathbf{g}} + M_{13} \hat{\mathbf{w}} \tag{4.27}$$

$$\begin{aligned} \frac{\partial h}{\partial \dot{\mathbf{r}}} &= Gn^{-1}a^{-2} \left[\left(\frac{\partial X_1}{\partial k} - h\beta \frac{\dot{X}_1}{n} \right) \hat{\mathbf{f}} + \left(\frac{\partial Y_1}{\partial k} - h\beta \frac{\dot{Y}_1}{n} \right) \hat{\mathbf{g}} \right] \\ &\quad + k(qY_1 - pX_1)n^{-1}a^{-2}G^{-1}\hat{\mathbf{w}} \\ &= M_{21}\hat{\mathbf{f}} + M_{22}\hat{\mathbf{g}} + M_{23}\hat{\mathbf{w}} \end{aligned} \tag{4.28}$$

$$\begin{aligned} \frac{\partial k}{\partial \dot{\mathbf{r}}} &= -Gn^{-1}a^{-2} \left[\left(\frac{\partial X_1}{\partial h} + k\beta \frac{\dot{X}_1}{n} \right) \hat{\mathbf{f}} + \left(\frac{\partial Y_1}{\partial h} + k\beta \frac{\dot{Y}_1}{n} \right) \hat{\mathbf{g}} \right] \\ &\quad - h(qY_1 - pX_1)n^{-1}a^{-2}G^{-1}\hat{\mathbf{w}} \\ &= M_{31}\hat{\mathbf{f}} + M_{32}\hat{\mathbf{g}} + M_{33}\hat{\mathbf{w}} \end{aligned} \tag{4.29}$$

$$\frac{\partial p}{\partial \dot{\mathbf{r}}} = KY_1 \frac{n^{-1}a^{-2}G^{-1}}{2} \hat{\mathbf{w}} = M_{41}\hat{\mathbf{f}} + M_{42}\hat{\mathbf{g}} + M_{43}\hat{\mathbf{w}} \tag{4.30}$$

$$\frac{\partial q}{\partial \dot{\mathbf{r}}} = KX_1 \frac{n^{-1}a^{-2}G^{-1}}{2} \hat{\mathbf{w}} = M_{51}\hat{\mathbf{f}} + M_{52}\hat{\mathbf{g}} + M_{53}\hat{\mathbf{w}} \tag{4.31}$$

$$\begin{aligned} \frac{\partial \lambda}{\partial \dot{\mathbf{r}}} &= n^{-1}a^{-2} \left[-2X_1 + G \left(h\beta \frac{\partial X_1}{\partial h} + k\beta \frac{\dot{X}_1}{\partial k} \right) \right] \hat{\mathbf{f}} \\ &\quad + n^{-1}a^{-2} \left[-2Y_1 + G \left(h\beta \frac{\partial Y_1}{\partial h} + k\beta \frac{\dot{Y}_1}{\partial k} \right) \right] \hat{\mathbf{g}} + n^{-1}a^{-2}G^{-1}(qY_1 - pX_1)\hat{\mathbf{w}} \\ &= M_{61}\hat{\mathbf{f}} + M_{62}\hat{\mathbf{g}} + M_{63}\hat{\mathbf{w}} \end{aligned} \tag{4.32}$$

where $\beta = 1/(1 + G)$, $G = (1 - h^2 - k^2)^{1/2}$, $K = 1 + p^2 + q^2$, $r = a(1 - kc_F - hs_F)$ with $(\hat{\mathbf{f}}, \hat{\mathbf{g}}, \hat{\mathbf{w}})$ representing the equinoctial frame and with the position and velocity vectors given by

$$\mathbf{r} = X_1 \hat{\mathbf{f}} + Y_1 \hat{\mathbf{g}} \tag{4.33}$$

$$\dot{\mathbf{r}} = \dot{X}_1 \hat{\mathbf{f}} + \dot{Y}_1 \hat{\mathbf{g}} \tag{4.34}$$

and where

$$X_1 = a \left[(1 - h^2\beta) c_F + hk\beta s_F - k \right] \tag{4.35}$$

$$Y_1 = a \left[hk\beta c_F + (1 - k^2\beta) s_F - h \right] \tag{4.36}$$

$$\dot{X}_1 = a^2 nr^{-1} \left[hk\beta c_F - (1 - h^2\beta) s_F \right] \tag{4.37}$$

$$\dot{Y}_1 = a^2 nr^{-1} \left[(1 - k^2\beta) c_F - hk\beta s_F \right] \tag{4.38}$$

with F representing the eccentric longitude, which is obtained from Kepler’s equation by iteration

$$\lambda = F - ks_F + hc_F \tag{4.39}$$

Finally,

$$\frac{\partial X_1}{\partial h} = a \left[-(hc_F - ks_F) \left(\beta + \frac{h^2\beta^3}{(1 - \beta)} \right) - \frac{a}{r} c_F (h\beta - s_F) \right] \tag{4.40}$$

$$\frac{\partial X_1}{\partial k} = -a \left[(hc_F - ks_F) \frac{hk\beta^3}{(1 - \beta)} + 1 + \frac{a}{r} s_F (s_F - h\beta) \right] \tag{4.41}$$

$$\frac{\partial Y_1}{\partial h} = a \left[(hc_F - ks_F) \frac{hk\beta^3}{(1 - \beta)} - 1 + \frac{a}{r} c_F (k\beta - c_F) \right] \tag{4.42}$$

$$\frac{\partial Y_1}{\partial k} = a \left[(hc_F - ks_F) \left(\beta + \frac{k^2\beta^3}{(1 - \beta)} \right) + \frac{a}{r} s_F (c_F - k\beta) \right] \tag{4.43}$$

The equation for the mass is as before given by

$$\dot{m} = -\frac{f^2}{2P} = -\frac{2P}{c^2} = -\frac{f}{c}$$

The system equations can now be written as

$$\dot{\mathbf{z}} = \frac{f}{m} M(\mathbf{z}, F) \hat{\mathbf{u}} \tag{4.44}$$

$$\dot{m} = -\frac{f^2}{2P(\mathbf{z}, F, \hat{\mathbf{u}})} \tag{4.45}$$

Here, P is assumed to be a function of the vehicle orientation. Let us further assume that the thrust magnitude is not constrained, such that the Hamiltonian of the system above is written as

$$H = \lambda_z^T \cdot \dot{\mathbf{z}} + \lambda_m \dot{m} = \lambda_z^T \frac{f}{m} M(\mathbf{z}, F) \hat{\mathbf{u}} - \lambda_m \frac{f^2}{2P(\mathbf{z}, F, \hat{\mathbf{u}})} + \lambda_\lambda n \tag{4.46}$$

If P is not a function of $\hat{\mathbf{u}}$, then

$$H = \lambda_z^T \cdot \frac{f}{m} M(\mathbf{z}, F) \hat{\mathbf{u}} - \lambda_m \frac{f^2}{2P(\mathbf{z}, F)} + \lambda_\lambda n \tag{4.47}$$

H is maximized if $\hat{\mathbf{u}}$ is chosen parallel to $\lambda_z^T (f/m) M(\mathbf{z}, F)$ or

$$\hat{\mathbf{u}} = \frac{\lambda_z^T \frac{f}{m} M(\mathbf{z}, F)}{\left| \lambda_z^T \frac{f}{m} M(\mathbf{z}, F) \right|} \tag{4.48}$$

Then, H is reduced to

$$H = \left| \lambda_z^T \frac{f}{m} M(\mathbf{z}, F) \right| - \lambda_m \frac{f^2}{2P(\mathbf{z}, F)} + \lambda_\lambda n \tag{4.49}$$

and the optimal thrust magnitude is obtained from the optimality condition $\partial H/\partial f = 0$, which results in

$$f^* = \frac{|\lambda_z^T M(\mathbf{z}, F)| P(\mathbf{z}, F)}{\lambda_m m} \quad (4.50)$$

This is equivalent to the maximization of

$$f + \frac{m\lambda_m}{|\lambda_z^T M(\mathbf{z}, F)|} \dot{m} = \max \quad (4.51)$$

because \dot{m} is equal to $-f^2/2P$ in Equation (4.49). Equation (4.50) is identical to Equation (4.24), where the \mathbf{r}, \mathbf{v} formulation was used. Here, $|\lambda_z^T M(\mathbf{z}, F)|$ replaces λ_v , because the state variables are the equinoctial elements. Equation (4.51) is the equation of the straight line in the $(f, -\dot{m})$ system, and the maximum takes place when the line is tangent to the P_{\max} curve (Figure 4.4), such as at point 1. At a later time, the optimal operating point is at 2, with f_2^* representing the optimal time-varying thrust magnitude [1, 3].

The corresponding mass flow rate at each instant of time is, of course, obtained from $\dot{m} = -f^2/2P$, and the optimal I_{sp}^* from

$$I_{\text{sp}}^* = \frac{2m\lambda_m}{g |\lambda_z^T M(\mathbf{z}, F)|} \quad (4.52)$$

The Euler–Lagrange differential equations are given by

$$\dot{\lambda}_z^T = -\frac{\partial H}{\partial \mathbf{z}} = -\lambda_z^T \frac{\partial M}{\partial \mathbf{z}} \frac{f}{m} \hat{\mathbf{u}} - \lambda_\lambda \frac{\partial n}{\partial \mathbf{z}} \quad (4.53)$$

$$\dot{\lambda}_m = -\frac{\partial H}{\partial m} = \lambda_z^T M \frac{f}{m^2} \hat{\mathbf{u}} \quad (4.54)$$

where it is assumed that the power P is independent of the state vector \mathbf{z} , being considered constant throughout the transfer. The $\partial M/\partial \mathbf{z}$ partials have been derived in [7] and in Chapter 3 of this book, and are not repeated here.

For the optimization of the thrust orientation, the maximum principle is used to get

$$\hat{\mathbf{u}} = \frac{(\lambda_z^T M)^T}{|\lambda_z^T M|} \quad (4.55)$$

and thereby the three components u_f , u_g and u_w , which in turn provide the values of u_r , u_θ and u_h in the rotating $\hat{\mathbf{r}}, \hat{\boldsymbol{\theta}}, \hat{\mathbf{h}}$ frame. The instantaneous pitch and yaw angles are obtained from $\theta_t = \tan^{-1}(u_r/u_\theta)$ and $\theta_h = \tan^{-1}(u_h/u_\theta)$, as in [7] and in Chapter 3 of this book.

If the thrust magnitude is unconstrained, its optimal value is obtained from the optimality condition

$$\frac{\partial H}{\partial f} = 0 = \lambda_z^T \frac{M}{m} \hat{\mathbf{u}} - \frac{f}{P} \lambda_m \quad (4.56)$$

which yields the optimal thrust f^* :

$$f^* = \frac{P (\lambda_z^T M \hat{\mathbf{u}})^T}{m\lambda_m} \quad (4.57)$$

The optimal value of the specific impulse is then given by

$$I_{sp}^* = \frac{2P}{f^*g} \quad (4.58)$$

because $c = 2P/f = I_{sp}g$. Now the optimal acceleration program is obtained from

$$f_t^* = \frac{f^*}{m} = \frac{\lambda_z^T M \hat{\mathbf{u}}}{m^2 \lambda_m} P \quad (4.59)$$

If the thrust magnitude is bounded from above and below, then

$$f_{\min} < f < f_{\max} \quad (4.60)$$

such that we have the following inequality constraints on the control variable f

$$C_1 = f - f_{\max} \leq 0 \quad (4.61)$$

$$C_2 = -f + f_{\min} \leq 0 \quad (4.62)$$

These constraints can be adjoined to the original Hamiltonian by way of Lagrange multipliers, μ_1 and μ_2 such that

$$H = \frac{f}{m} \lambda_z^T M \hat{\mathbf{u}} - \frac{f^2}{2P} \lambda_m + \lambda_\lambda n + \mu_1 (f - f_{\max}) + \mu_2 (-f + f_{\min}) \quad (4.63)$$

The necessary condition on H is

$$H_f = \frac{\partial H}{\partial f} = \lambda_z^T \frac{M}{m} \hat{\mathbf{u}} - \frac{f}{P} \lambda_m + \mu_1 - \mu_2 = 0 \quad (4.64)$$

The multipliers μ_1 and μ_2 are such that $\mu_1 > 0$ when $C_1 = 0$ or $f = f_{\max}$, and $\mu_1 = 0$ when $C_1 < 0$ or $f < f_{\max}$, and similarly $\mu_2 > 0$ when $C_2 = 0$ or $f = f_{\min}$, and $\mu_2 = 0$ when $C_2 < 0$ or $f > f_{\min}$. When $f_{\min} < f < f_{\max}$ assumes an intermediate value, $\mu_1 = \mu_2 = 0$, and $H_f = 0$ reduces to $\lambda_z^T (M/m) \hat{\mathbf{u}} - (f/P) \lambda_m = 0$, yielding the optimal control given by Equation (4.57). The values of μ_1 and μ_2 are readily obtained from

$$\mu_1 = \frac{f_{\max}}{P} \lambda_m - \frac{\lambda_z^T M \hat{\mathbf{u}}}{m} \quad (4.65)$$

$$\mu_2 = -\frac{f_{\min}}{P} \lambda_m + \frac{\lambda_z^T M \hat{\mathbf{u}}}{m} \quad (4.66)$$

The Lagrange multipliers are still given by Equations (4.53) and (4.54), and the optimal f^* is selected by monitoring the value of $\lambda_z^T M \hat{\mathbf{u}} P / (m \lambda_m)$. If it is less than f_{\min} , then we use $f^* = f_{\min}$, and if it is larger than f_{\max} , then we use, $f = f_{\max}$, and finally, if it is intermediate between f_{\min} and f_{\max} then we use f^* as given by Equation (4.57), which is the presently calculated value of $\lambda_z^T M \hat{\mathbf{u}} P / (m \lambda_m)$.

We can also use the simpler Hamiltonian H^* without adjoining the constraints, namely

$$H^* = \lambda_z^T \dot{\mathbf{z}} + \lambda_\lambda \dot{m} = \frac{f}{m} \left(\lambda_z^T M \hat{\mathbf{u}} - \frac{m \lambda_m}{c} \right) + \lambda_\lambda n \quad (4.67)$$

This is equivalent to Equation (4.68) because $c = 2P/f$ is a function of the control f :

$$H^* = \frac{f}{m} \lambda_z^T M \hat{\mathbf{u}} - \frac{f^2}{2P} \lambda_m + \lambda_\lambda n \tag{4.68}$$

The optimality condition yields, with

$$\frac{\partial H^*}{\partial f} = H_f^* = \lambda_z^T \frac{M}{m} \hat{\mathbf{u}} - \frac{f}{P} \lambda_m \tag{4.69}$$

the following relation

$$\delta H^* = H_f^* \delta f \leq 0 \tag{4.70}$$

because this is equivalent to

$$\delta J = \int_{t_0}^{t_f} H_f^* \delta f dt = \int_{t_0}^{t_f} \delta H^* dt \leq 0$$

for the control f to be maximizing for all admissible values of δf . δJ is the variation in J , the performance index, due to variations in f , for fixed $\mathbf{z}(t_0)$. The optimal control is selected by monitoring the value of H_f^* . If H_f^* as calculated by Equation (4.69) is positive, then we use $f = f_{\max}$, and if H_f^* is negative we use $f = f_{\min}$ and, finally, if $H_f^* = 0$, then we use f^* from Equation (4.69):

$$H_f^* > 0 \Rightarrow \delta f < 0 \Rightarrow f = f_{\max} \tag{4.71}$$

$$H_f^* < 0 \Rightarrow \delta f > 0 \Rightarrow f = f_{\min} \tag{4.72}$$

$$H_f^* = 0 \Rightarrow f = f^* = \lambda_z^T \frac{M \hat{\mathbf{u}}}{m \lambda_m P} \tag{4.73}$$

In practice, the last condition for $H_f^* = 0$ is replaced by $|H_f^*| < \varepsilon$, where, ε is a small number, say, 10^{-10} . The Euler–Lagrange equations are still given by Equations (4.53) and (4.54).

4.3 A Simple Example of Rendezvous in Near-Circular Orbit

Let us revisit our rendezvous example of [7], also shown in the previous chapter, in which a minimum-time solution with a continuous constant acceleration was generated. The mass equation was not used in [7] because the acceleration vector assumed effectively the role of the control, and it was then sufficient to optimize its direction to achieve the minimum-time solution. Under these assumptions, this solution was also equivalent to the minimum-fuel solution as was demonstrated in [8] and also discussed in the previous chapter, in which the mass equation was used, and the minimum-fuel time-fixed problem formulated using the same set of equinoctial nonsingular orbit elements. For a given initial mass $m_0 = 6000$ kg and a constant $I_{sp} = 3800$ s, an equivalent power of $P = 39,112.3$ W was used in order to obtain an average acceleration of $f_t = 3.5 \times 10^{-7}$ km/s², equal to the value of the constant acceleration used in [7] and Chapter 3 of this book. We now attempt to solve the same problem by allowing the I_{sp} to vary in order to improve the fuel consumption. As in [8] and Chapter 3 of this book, we maximize the

value of the mass at the fixed final time t_f , such that the performance index $J = \phi = m_f$, with the optimal thrust direction given by Equation (4.55) obtained directly from the maximum principle. Because the equations of motion given by Equations (4.44) and (4.45) are not explicit functions of time, the Hamiltonian H in Equation (4.46) or H^* in Equation (4.68) is constant throughout the transfer. Given initial state parameters $(a)_0$, $(h)_0$, $(k)_0$, $(p)_0$, $(q)_0$, $(\lambda)_0$ and $(m)_0$, the initial values of the seven Lagrange multipliers are guessed, namely $(\lambda_a)_0$, $(\lambda_h)_0$, $(\lambda_k)_0$, $(\lambda_p)_0$, $(\lambda_q)_0$, $(\lambda_\lambda)_0$, $(\lambda_m)_0$, and the state adjoint equations given by Equations (4.44), (4.45) and (4.53), (4.54) integrated forward from $t_0 = 0$ to $t_f = 86,402.453$ s, by using the optimal thrust direction $\hat{\mathbf{u}}$ in Equation (4.55), and the thrust magnitude from Equations (4.71), (4.72) and (4.73). The initial values of the multipliers are iterated until the desired terminal state given by $(a)_f$, $(h)_f$, $(k)_f$, $(p)_f$, $(q)_f$, $(\lambda)_f$ and $(m)_f = (\partial\phi/\partial m)_{t_f} = 1$ are satisfied. This is achieved by minimizing the following objective function:

$$F' = w_1 [a - (a)_f]^2 + w_2 [h - (h)_f]^2 + w_3 [k - (k)_f]^2 + w_4 [p - (p)_f]^2 + w_5 [q - (q)_f]^2 + w_6 [\lambda - (\lambda)_f]^2 + w_7 [\lambda_m - 1]^2 \quad (4.74)$$

where w_j are certain weights, and where the values of a , h , k , p , q , λ and λ_m are evaluated at the fixed terminal time t_f . Let $a_0 = 42,000,000$ m, $e_0 = 0$, $i_0 = 28.5$ deg, $\Omega_0 = 30$ deg, $\omega_0 = 10$ deg, $M_0 = 0$ deg, $m_0 = 6000$ kg, $P_0 = 40,000$ W, and $a_f = 42,767,073$ m, $e_f = 1.64459 \times 10^{-4}$, $i_f = 28.343$ deg, $\Omega_f = 29.999$ deg, $\omega_f = 247.299$ deg, $M_f = 120.905$ deg, and $t_f = 86,402.453$ s. Because the power is assumed to remain constant, let us select $(I_{sp})_{\min} = 3000$ s and $(I_{sp})_{\max} = 4000$ s, such that

$$f_{\min} = \frac{2P}{(I_{sp})_{\max} g} = \frac{2 \times 40,000}{4000 \times 9.80665} = 2.039432 \text{ N}$$

$$f_{\max} = \frac{2P}{(I_{sp})_{\min} g} = 2.719243 \text{ N}$$

The values of f_{\max} and f_{\min} are used as input to the optimizer, and they correspond to initial accelerations of $(f_t)_{\max} = f_{\max}/m_0 = 2.719243/6000 = 4.532071 \times 10^{-4}$ m/s², and $(f_t)_{\min} = f_{\min}/m_0 = 2.039432/6000 = 3.399053 \times 10^{-4}$ m/s², or an average of 3.965562×10^{-4} m/s², or 3.965562×10^{-7} km/s², which is slightly higher than the constant $f_t = 3.5 \times 10^{-7}$ km/s² used in [7] and duplicated in [8] and the previous chapter, by adjusting the power accordingly. Here we leave the power at 40,000 W, so that the I_{sp} bounds are exactly at the $(I_{sp})_{\min}$ and $(I_{sp})_{\max}$ values. Furthermore, the acceleration being now variable, it will be optimized to achieve minimum-fuel consumption. The solution is given by $(\lambda_a)_0 = 1.05651899 \times 10^{-5}$, $(\lambda_h)_0 = -3.102865136$, $(\lambda_k)_0 = 3.077180522$, $(\lambda_p)_0 = -5.066278561 \times 10^{-2}$, $(\lambda_q)_0 = -8.672939167 \times 10^{-2}$, $(\lambda_\lambda)_0 = -2.160048598$, $(\lambda_m)_0 = 0.9984527097$, where the various λ s have units that are the inverse of the corresponding element rates, namely s/m for λ_a , s/rad for λ_λ and s/kg for λ_m , with the remaining λ units being seconds because h , k , p and q are unitless. This is needed because the Hamiltonian is unitless.

The initial values of the elements are $a_0 = 4.2 \times 10^7$ m, $h_0 = 0$, $k_0 = 0$, $p_0 = 1.269838 \times 10^{-1}$, $q_0 = 2.199424 \times 10^{-1}$, $\lambda_0 = 6.981317 \times 10^{-1}$ rad, and

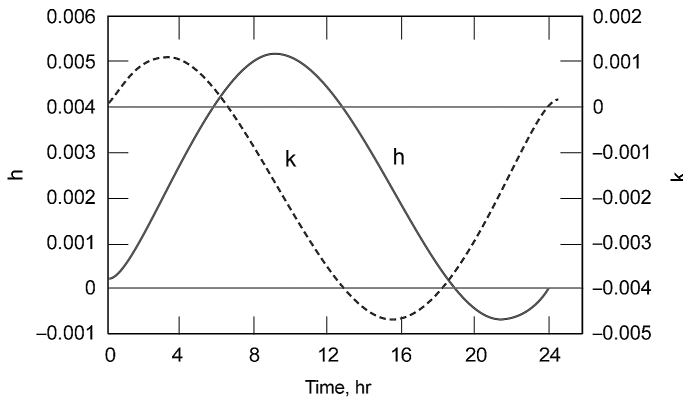


Figure 4.5 Variation of h and k on an optimal trajectory.

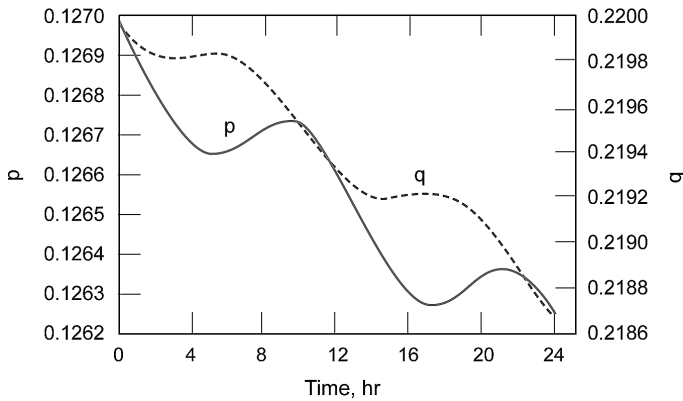


Figure 4.6 Variation of p and q on an optimal trajectory.

$m_0 = 6000$ kg. The final achieved parameters are $a = 42,767,073$ m, $e = 1.64459 \times 10^{-4}$, $i = 28.343$ deg, $\Omega = 29.999$ deg, $\omega = 247.299$ deg, $M = 120.905$ deg, $m_f = 5995.251893$ kg and $\lambda_m = 1.000000000$, indicating a local optimum. The Hamiltonian stays constant at $H = -0.959 \times 10^{-4}$ or essentially near zero. Figures 4.5–4.7 show the variations of h , k , p , q , H , and λ as a function of time, while Figures 4.8–4.10 depict the variations of the classical orbit elements. Figures 4.11–4.14 show how λ_a , λ_λ , λ_h , λ_k , λ_p , λ_q , m and λ_m vary during the optimal transfer. The terminal mass $m_f = 5995.251893$ kg is as expected, higher than the final mass of 5995.022 kg obtained with a constant $I_{sp} = 3800$ s in [8] and Chapter 3 of this book, showing the benefit of using a variable I_{sp} , and resulting in a decrease in fuel consumption of 0.229 kg. Figure 4.15 shows the optimal thrust orientation given by the pitch and yaw angles θ_t and θ_h , while Figure 4.16 depicts the acceleration program as well as the I_{sp} as a function of time. There are two arcs of constant maximum I_{sp} in this particular example.

Now if we relax the I_{sp} bounds or, equivalently, the thrust bounds, we could generate a trajectory that uses only intermediate thrust levels. Let $(I_{sp})_{min} = 1000$ s, and $(I_{sp})_{max} = 10,000$ s, or equivalently $(f)_{min} = 8.157729 \times 10^{-1}$ N, and $(f)_{max} = 8.157729$ N

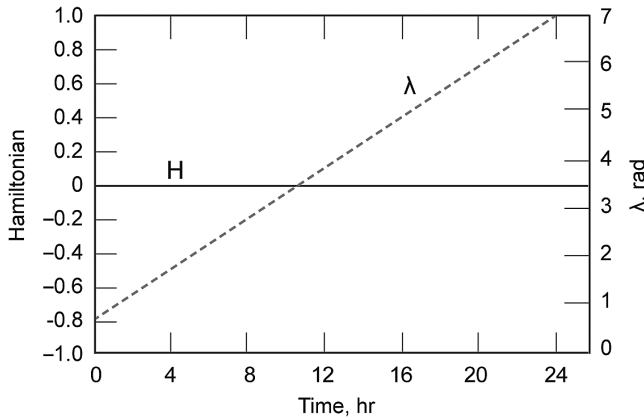


Figure 4.7 Variation of λ and H on optimal Hamiltonian.

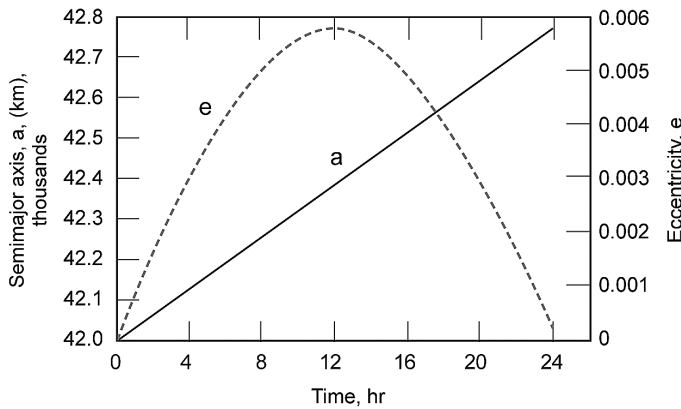


Figure 4.8 Evolution of a and e on an optimal rendezvous trajectory.

for our example at hand. The solution is given by $(\lambda_a)_0 = 1.087325882 \times 10^{-5}$, $(\lambda_h)_0 = -4.548851268$, $(\lambda_k)_0 = 4.130745710$, $(\lambda_p)_0 = -5.080206079 \times 10^2$, $(\lambda_q)_0 = -8.719703291 \times 10^2$, $(\lambda_\lambda)_0 = -2.630702853$, $(\lambda_m)_0 = 0.9984192335$, with $m_f = 5995.255825$ kg, which is only slightly higher than the value obtained in the example above. Figure 4.17 shows the acceleration program as well as the I_{sp} time history, which remains at intermediate values never reaching either the minimum or maximum bounds. This solution represents therefore the thrust magnitude unconstrained case providing the overall minimum-fuel expenditure. As a final example, let $(I_{sp})_{min} = 3700$ s and $(I_{sp})_{max} = 4000$ s, such that the transfer must now use a smaller I_{sp} bandwidth than our first example. These bounds correspond to $(f)_{min} = 2.039432$ N, and $(f)_{max} = 2.204791$ N, and the solution is given by $(\lambda_a)_0 = 1.058971845 \times 10^{-5}$, $(\lambda_h)_0 = -3.140806779$, $(\lambda_k)_0 = 3.401400619$, $(\lambda_p)_0 = -5.071540433 \times 10^2$, $(\lambda_q)_0 = -8.679605832 \times 10^2$, $(\lambda_\lambda)_0 = -2.307546419$, $(\lambda_m)_0 = 0.9984514728$, with the final mass at $m_f = 5995.251875$ kg. This value is slightly less than the corresponding

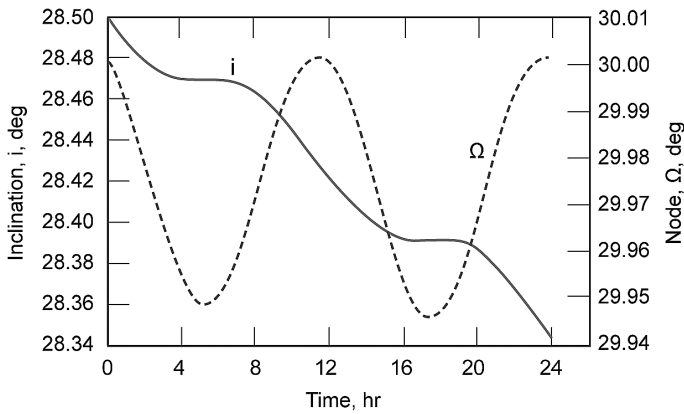


Figure 4.9 Evolution of i and Ω on an optimal rendezvous trajectory.

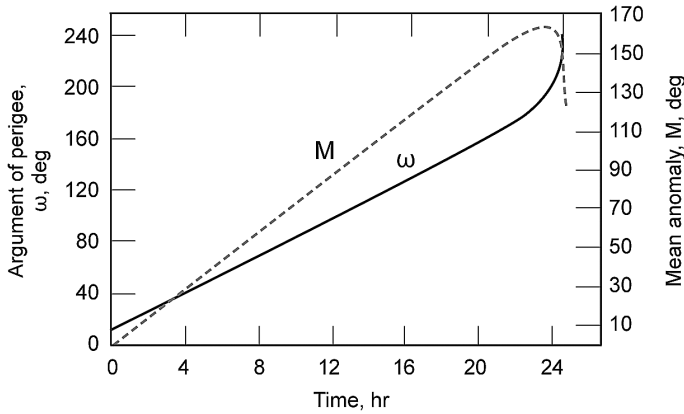


Figure 4.10 Evolution of M and ω on an optimal rendezvous trajectory.

value obtained for the absolute minimum-fuel transfer of 5995.255825 kg with unconstrained thrust magnitude, and also slightly less than the value of 5995.251893 kg of the first example. This is because, in this last example, both minimum I_{sp} and maximum I_{sp} thrust arcs are generated as shown in Figure 4.18 due to the narrowing of the I_{sp} bandwidth, which further constrains the transfer. These examples validate the analytical developments and verify that the code is error-free, because the correct trends are clearly appearing, even though the savings in fuel are very small for this particular rendezvous trajectory. The final state is met with a very small tolerance in order to produce the exact trajectories for a meaningful comparison. Substantial savings in fuel are possible especially with the higher values of specific power, or power to mass ratio, for highly elliptical orbit transfers and for larger changes in the energy and angular momentum vector.

Furthermore, because the thrust is continuously on, or otherwise the control is continuous, it is much easier to generate a series of transfers with increasing I_{sp} bandwidths,

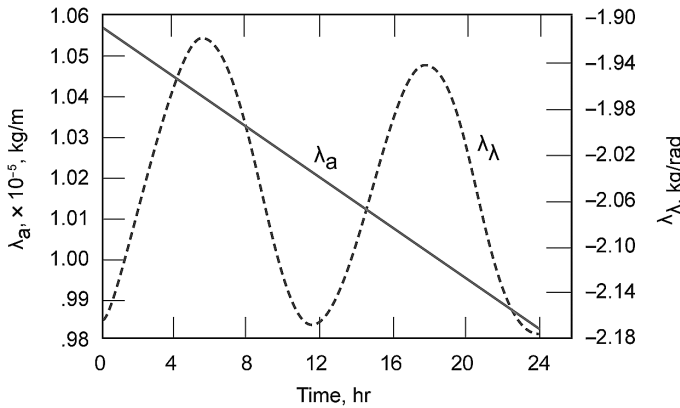


Figure 4.11 λ_a and λ_λ versus time.

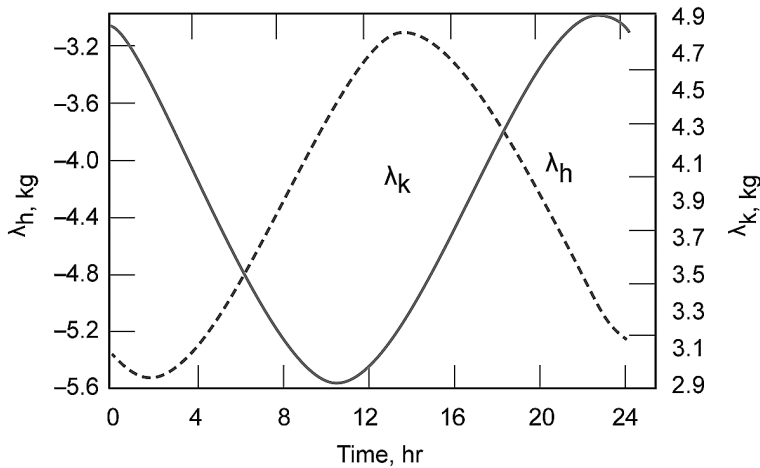


Figure 4.12 λ_h and λ_k versus time.

such that, in the limit, the discontinuous thrust case can be produced with full thrust cut-off arcs, which correspond to infinite I_{sp} or, in practice, negligible thrust. These coast arcs are beneficial for certain transfer geometries, especially, if the fixed transfer time is further relaxed from its minimum-time value obtained with continuous thrust. Finally, when a given engine design is used with specified I_{sp} bounds, the thrust magnitude unconstrained solution may not be possible to fly due to the engine limitations, which in turn will necessitate the generation of the optimal I_{sp} -constrained solution as shown in these examples.

4.4 Conclusion

The use of the variation of parameters equations based on a set of nonsingular equinoctial orbit elements is extended to the important case of minimum-fuel time-fixed transfer

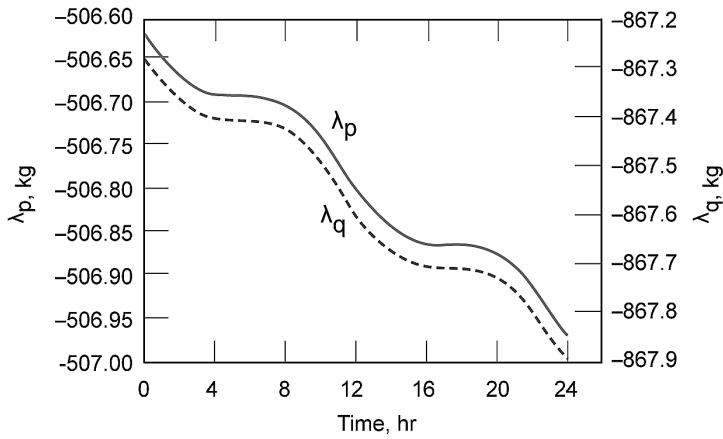


Figure 4.13 λ_p and λ_q versus time.

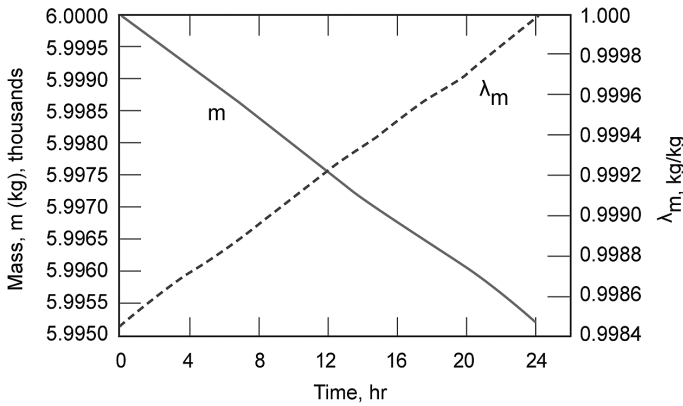


Figure 4.14 λ_m and m versus time.

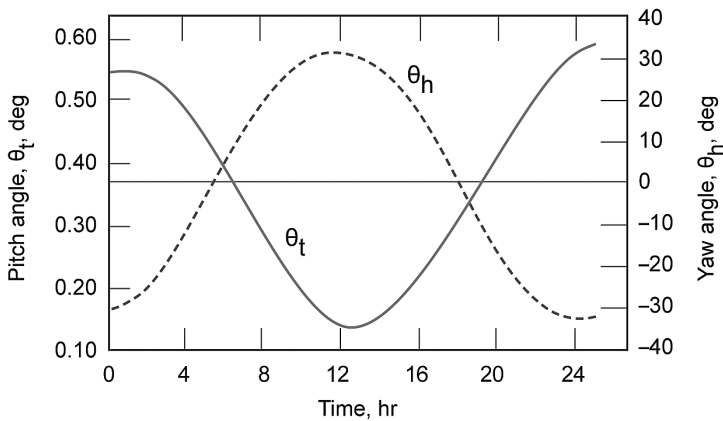


Figure 4.15 Optimal thrust pitch and yaw program.

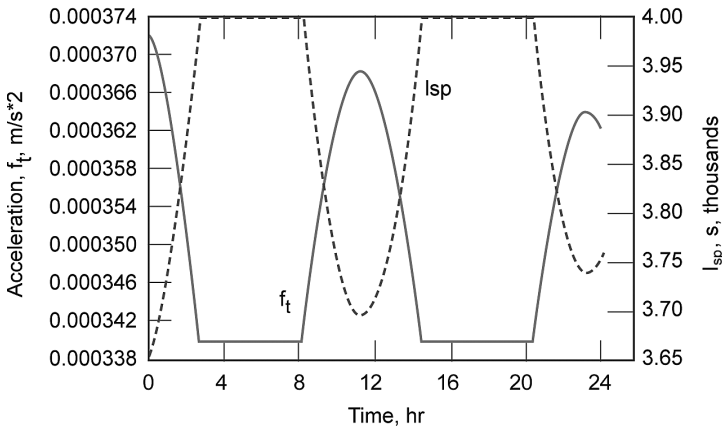


Figure 4.16 Optimal acceleration and I_{sp} program with $(I_{sp})_{max} = 4000$ s and $(I_{sp})_{min} = 3000$ s.

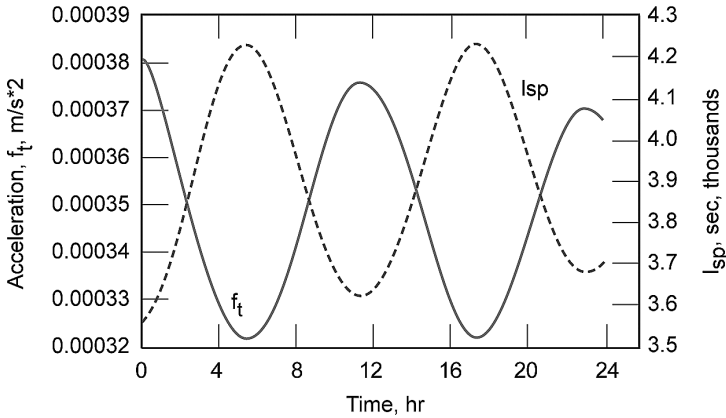


Figure 4.17 Optimal acceleration and I_{sp} program with $(I_{sp})_{max} = 10,000$ s and $(I_{sp})_{min} = 1000$ s.

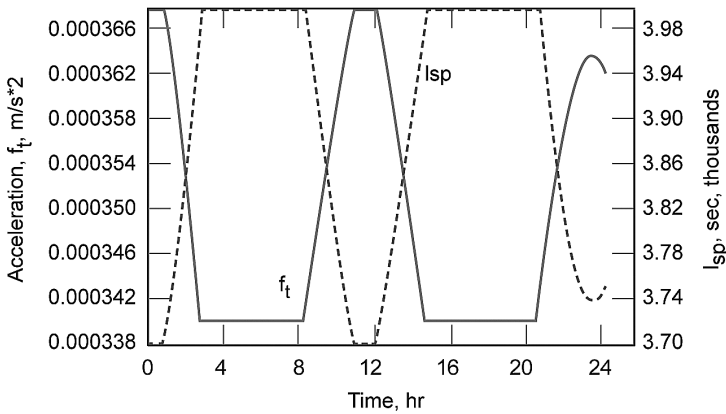


Figure 4.18 Optimal acceleration and I_{sp} program with $(I_{sp})_{max} = 4000$ s and $(I_{sp})_{min} = 3700$ s.

and rendezvous, where both thrust magnitude and orientation are simultaneously optimized. Furthermore, minimum and maximum bounds on the thrust magnitude, or equivalently I_{sp} , are considered in order to allow the throttling of the propulsion system, which in turn can result in substantial savings in propellant consumption, especially when the fixed flight time is further relaxed. The limiting case of coasting arcs can be approached by increasing the maximum I_{sp} bound, such that the discontinuous control transfer problem can later be solved after the proper thrust–coast sequence is essentially guessed using the simpler and more robust continuous control algorithm developed in this chapter.

References

- [1] Edelbaum, T. N. (1969) *Optimal Space Trajectories*, Analytic Mechanics Associates Inc., Jericho, NY.
- [2] Hill, P. G. and Peterson, C. R. (1970) *Mechanics and Thermodynamics of Propulsion*, Addison-Wesley, New York, NY.
- [3] Marec, J.-P. (1979) *Optimal Space Trajectories*, Elsevier, Amsterdam.
- [4] Vinh, N. X. (1981) *Optimal Trajectories in Atmospheric Flight*, Elsevier, Amsterdam.
- [5] Bryson, A. E. and Ho, Y.-C. (1969) *Applied Optimal Control*, Ginn, Waltham, MA.
- [6] Edelbaum, T. N., Sackett, L. L. and Malchow, H. L. (1973) *Optimal Low Thrust Geocentric Transfer*, AIAA Paper 73–1074, AIAA 10th Electric Propulsion Conference, Lake Tahoe, NV.
- [7] Kechichian, J. A. (1992) *Optimal Low-Thrust Rendezvous Using Equinoctial Orbit Elements*, IAF Paper 92–0014, 43rd Congress of the International Astronautical Federation, Washington, DC.
- [8] Kechichian, J. A. (1993) *Minimum-Fuel Time-Fixed Rendezvous Using Constant Low-Thrust*, AAS Paper 93–130, AAS/AIAA Spaceflight Mechanics Meeting, Pasadena, CA.